CrossMark

ORIGINAL ARTICLE

Fiducial-based registration with a touchable region model

Sungmin Kim[1] · Peter Kazanzides[1]

Abstract

Purpose Image-guided surgery requires registration between an image coordinate system and an intraoperative coordinate system that is typically referenced to a tracking device. In fiducial-based registration methods, this is achieved by localizing points (fiducials) in each coordinate system. Often, both localizations are performed manually, first by picking a fiducial point in the image and then by using a hand-held tracked pointer to physically touch the corresponding fiducial on the patient. These manual procedures introduce localization error that is user-dependent and can significantly decrease registration accuracy. Thus, there is a need for a registration method that is tolerant of imprecise fiducial localization in the preoperative and intraoperative phases.

Methods We propose the iterative closest touchable point (ICTP) registration framework, which uses model-based localization and a touchable region model. This method consists of three stages: (1) fiducial marker localization in image space, using a fiducial marker model, (2) initial registration with paired-point registration, and (3) fine registration based on the iterative closest point method.

Results We perform phantom experiments with a fiducial marker design that is commonly used in neurosurgery. The results demonstrate that ICTP can provide accuracy improvements compared to the standard paired-point registration method that is widely used for surgical navigation and surgical robot systems, especially in cases where the surgeon introduces large localization errors.

Conclusions The results demonstrate that the proposed method can reduce the effect of the surgeon's localization performance on the accuracy of registration, thereby producing more consistent and less user-dependent registration outcomes.

Keywords Registration · Fiducial marker · Surgical navigation · Surgical robot

Introduction

Stereotactic surgery is a surgical technique that uses medical image data and a three-dimensional coordinate system to localize a target inside the body and to guide an intervention. Stereotactic surgery can be categorized as frame based or frameless, depending on how the reference coordinate system is obtained. Frame-based stereotactic surgery provides a reference coordinate system by fixing a physical frame on the patient [11], whereas frameless stereotactic surgery instead uses a surgical global positioning system (SGPS) and a registration method to determine the spatial relationship between the patient and the SGPS [5]. This registration method commonly relies on fiducial markers that are placed prior to the acquisition of preoperative CT or MRI. This enables the surgeon to localize the fiducials in the image data. Intraoperatively, the surgeon can obtain another point set by using a tracked instrument to digitize the fiducial markers. These two point sets are registered, typically using a paired-point registration method, to obtain the transformation between the image coordinate system and the SGPS coordinate system.

An alternate approach is to rely on anatomical features instead of implanted fiducials. In some cases, anatomical features can be precisely localized both in the image and

✉ Sungmin Kim
   sungminkim@jhu.edu

   Peter Kazanzides
   pkaz@jhu.edu

[1] Department of Computer Science, Johns Hopkins University, Baltimore, MD 21218, USA

intraoperatively and thus can directly replace implanted fiducials in a paired-point registration framework. However, a more robust and widely adopted approach is to digitize a set of points on the anatomy and then use an optimization method, typically iterative closest point (ICP) [2], to register this intraoperative point set to a surface model of the anatomy created by segmenting the preoperative image. Numerous improvements to the standard ICP algorithm have been proposed, including a few that focus on adopting more general noise models (beyond isotropic Gaussian noise) [3,9].

The focus of this work is on paired-point registration with implanted fiducials, as this method is widely used in areas such as image-guided neurosurgery. To obtain high registration accuracy, several factors must be considered, including: (1) the accuracy of fiducial localization in image space, (2) the accuracy of fiducial localization in surgical space, and (3) the accuracy of the registration algorithm. To improve the registration accuracy, there have been ongoing efforts to reduce the errors due to the above three factors. One approach is to apply image processing algorithms to reduce the fiducial localization error in image space, either in an automatic or semiautomatic manner, and either based on volume data or based on surface data [4,6,10,13,14]. While much of the previous research has focused on localizing fiducial markers using parameterized geometric information such as curvature or centroid of the fiducial marker, some researchers have proposed a localization method using a fiducial marker model [4,10]. In our work, we adopt a model-based localization method as described in [4], with minor implementation differences such as using an initial normal vector. For improved intraoperative localization, an alternate approach is to design a better fiducial marker, such as by providing a divot to ensure that the digitizing tool makes contact at a distinct point [8].

In this work, we propose a registration framework to improve registration accuracy by combining the paired-point registration (PPR) and iterative closest point (ICP) methods, considering fiducial marker and touchable region models during the registration procedures. This approach, iterative closest touchable point (ICTP), bears some similarity to the registration algorithm using spotlights [7], where the spotlights indicate the regions of the anatomy that should be intraoperatively digitized. After the surgeon has digitized a point in each spotlight, the algorithm uses a subsampled area to find the closest points in the model within an ICP registration framework. Our method can be considered an extension of the spotlights concept to fiducial localization, where the spotlight is not defined by the anatomy but rather by the touchable region model associated with the fiducial marker.

To ensure feasibility in a surgical environment, the proposed ICTP framework does not impose unduly burdensome or time-consuming intraoperative tasks on the registration procedure. Specifically, we focused on these two factors: (1) The registration framework must use the same proce-

dures for point-based registration that have been widely applied for surgical navigation and surgical robots and (2) the registration framework should significantly improve the fiducial localization and registration result when compared to the conventional paired-point registration, especially when there is imprecise point localization by the user. One of the key consequences of the second factor is that the proposed method reduces the effect of user localization skill and performance on the accuracy of fiducial-based registration. The next sections describe the proposed method and demonstrate its performance in phantom experiments. The final sections discuss the results and future work.

Methods

The proposed ICTP registration method consists of three stages, shown in Fig. 1: (1) fiducial marker localization in image space, using a fiducial marker model, (2) initial registration with paired-point registration, and (3) fine registration with iterative closest point (ICP) [2]. It is implemented using VTK as a Python module for 3D Slicer [12]. We illustrate the above steps using the multimodal fiducial marker, MM3302 (Fig. 2-left), produced by IZI Medical Products, because it has been widely used for neurosurgical applications, but the methods generalize to other marker designs.

Model-based fiducial marker localization

We used 3D CAD software to design a model for the IZI fiducial marker (Fig. 2-middle), based on its specifications. Our method further requires definition of the *touchable region* of the fiducial marker, which is the total region where the digitizing tool could touch the fiducial marker during the intraoperative localization procedure. We denote the touchable region surface model by S_{TR}. For this particular design, it is straightforward to adjust the touchable region model based on the radius of the digitizing tool tip, as illustrated in Fig. 2 right. Specifically, $R_{TR} = R_{IR} - R_T$, where R_{TR} is the radius of the touchable region, R_{IR} is the radius of the inner region of the fiducial marker, and R_T is the radius of the end tip of the digitizing tool. Similarly, the touchable region is offset in the vertical direction by R_T, relative to the marker model.

Model-based fiducial marker localization in the image can be conducted by a semiautomatic method. First, the user manually selects an initial target point, $\mathbf{p_{Ti}}$, for each fiducial ($i = 1, \ldots, N_T$, where N_T is the number of fiducials). The initial normal vector for each fiducial, $\mathbf{u_{Ti}}$, can be determined at the same time. The normal can be obtained automatically (e.g., by estimating the normal from the underlying image feature) or manually by user input.

Next, the localization determines a more accurate position and orientation of the fiducial marker using a model-based
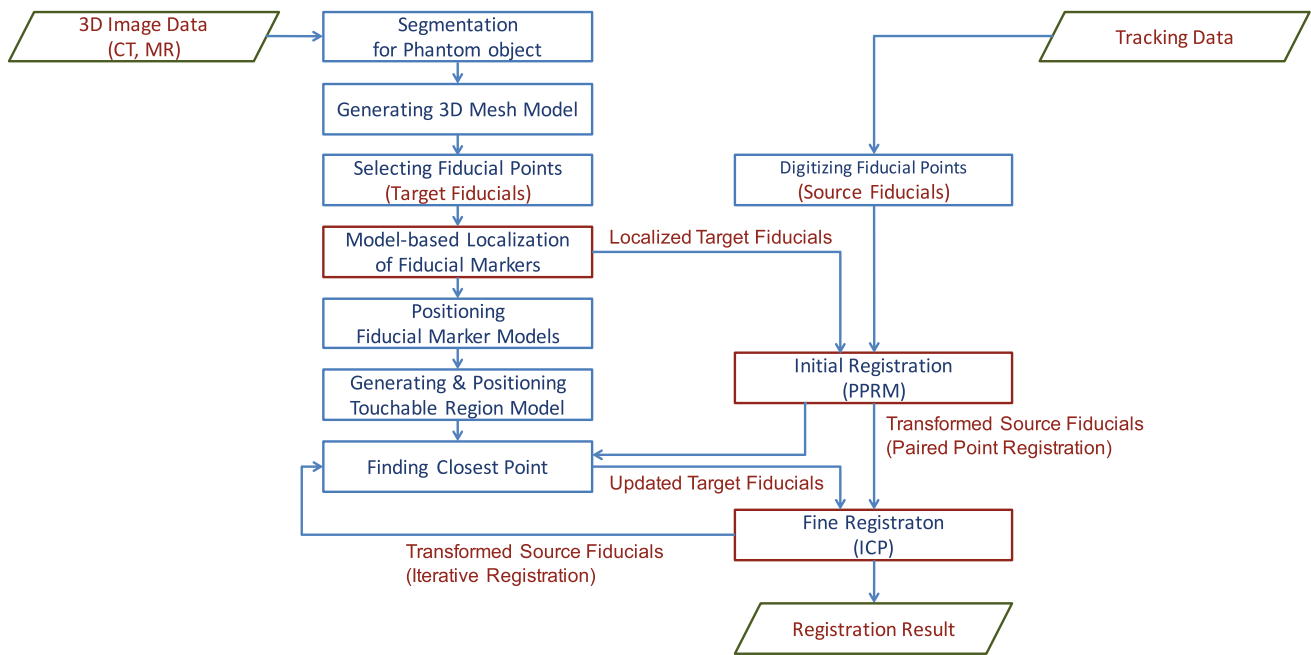
Fig. 1 Three major stages of the ICTP registration procedure (*red boxes*): fiducial marker localization, initial registration (PPRM), and fine registration (ICP)
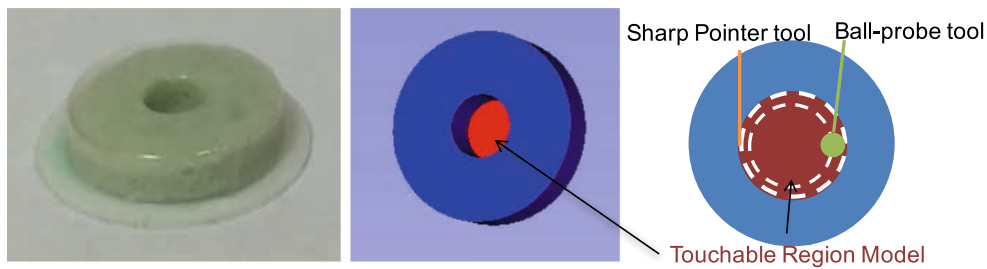

Fig. 2 Multimodal fiducial marker (*left*), the fiducial marker model designed via 3D CAD software (*middle*), and the touchable region model where the radius is based on the size of the tool tip; *outer* and *inner white dashed circles* designate the touchable regions for the sharp pointer and ball probe tools, respectively (*right*)

method, as described in [4]. In our current implementation, we assume that a patient model has been created from the preoperative image; at a minimum, the model should include the fiducials. We then use the iterative closest point (ICP) method (Fig. 3) to register the fiducial model (from CAD) to the patient model (from image), using the initial target points, $\mathbf{p_{Ti}}$, and normals, $\mathbf{u_{Ti}}$, to provide the initial transformation. Specifically, the vertices of the fiducial model serve as the point cloud and the patient model provides the surface. The result of applying the ICP method to each fiducial is a set of localization matrices, T_{Li}, that represent the transformation matrix between the fiducial marker coordinate system and the image coordinate system. If (by convention) the origin of the fiducial marker coordinate system is at the center of the fiducial, then the localized target point set, P_{LT}, is given by the translation component of each localization matrix.

Initial registration

The source point set P_S is collected intraoperatively with a tracked digitizing tool. The initial registration, T_I, is computed between the two point sets, P_{LT} and P_S, using a conventional (least squares) paired-point registration [1]:

$$T_I = \arg\min_{T_I} \sum_{i=1}^{N_T} \| \mathbf{p_{LTi}} - T_I \mathbf{p_{Si}} \|^2, \tag{1}$$

which is defined as paired-point registration with model-based localization (PPRM).

Finally, the transformed source point set P_{TS} can be computed by $P_{TS} = T_I P_S$ and used in the fine registration method below.

Fig. 3 Localizing fiducial markers in the image using the ICP method with the marker model, shown as flowchart (*left*) and graphical illustrations (*right*). Sequential steps are: (*top*) manual selection of initial fiducial points, followed by calculation of normal vectors, (*middle*) placement of fiducial marker model with respect to manually selected fiducial point and normal vector, (*bottom*) final localization with fiducial marker model. The *gray* model is the fiducial segmented from the image, and the *blue* model is the CAD design of the marker
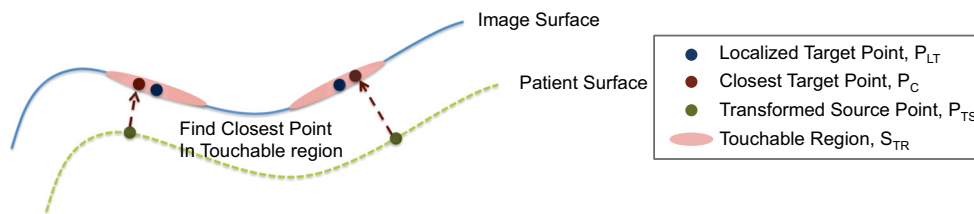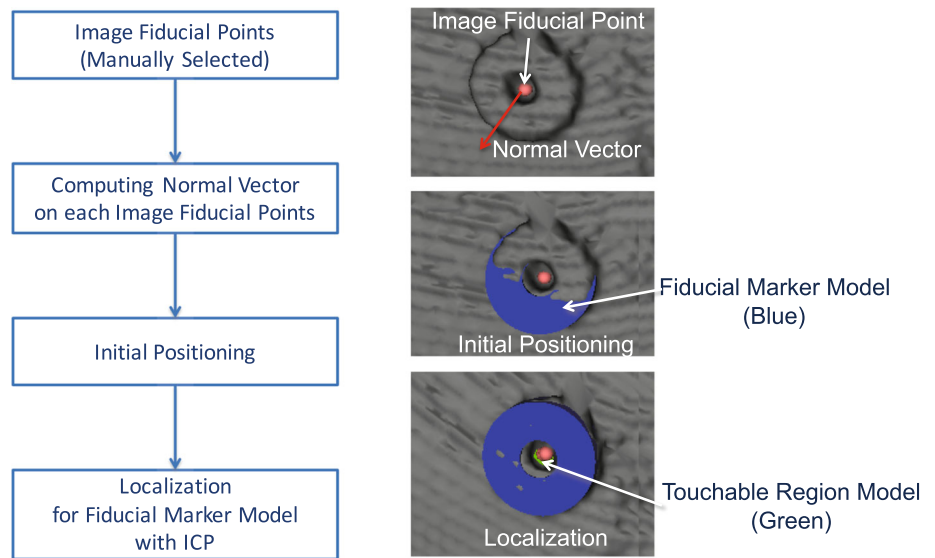
Fig. 4 Fine registration is conducted considering the touchable region on the fiducial marker during the iterative closest point step

Fine registration with touchable region model

The fine registration is implemented using the iterative closest point (ICP) method. In this case, however, the surface model actually consists of multiple surface patches, each corresponding to the touchable region of a fiducial marker. Because the correspondences between fiducial markers and touchable regions are known, the closest target point P_{Ci} can be found on the corresponding touchable region S_{TRi}, as shown in Fig. 4. The closest point $\mathbf{p_{Ci}}$ can be expressed as:

$$\mathbf{p_{Ci}} = \arg \min_{p_{TRi} \in S_{TRi}} d\left(\mathbf{p_{TSi}}, \mathbf{p_{TRi}}\right) \quad (2)$$

where p_{TRi} is a point in the ith touchable region S_{TRi} and $d(a, b)$ is the distance between two points, a and b. The ICP method is iterated until convergence, producing the registration matrix T_{ICP}:

$$T_{ICP} = \arg \min_{T_{ICP}} \sum_{i=1}^{N_T} \| P_C - T_{ICP} P_{TS} \|^2 \quad (3)$$

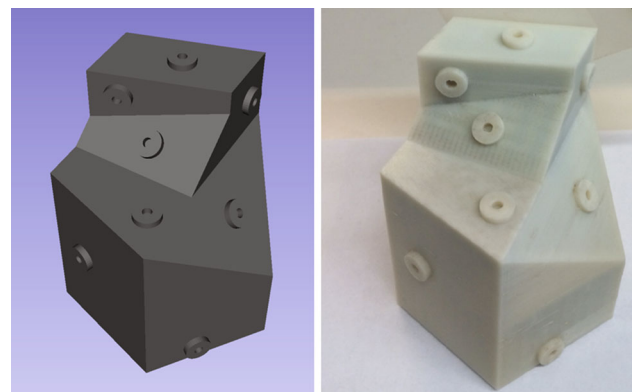The final transformation is given by $T_{ICP} T_I$.

Fig. 5 Phantom designed with 3D CAD software (*left*) and built via 3D printer (*right*)

Experiments

To evaluate the proposed registration method, a phantom with 10 fiducials was designed using 3D CAD software (the Solidworks, Dassault Systems) and built via a 3D printer (UPrint SE, Stratasys, Ltd), as shown in Fig. 5. The phantom was CT scanned with a voxel resolution of $0.35 \times 0.35 \times 0.8$ mm. In addition, synthetic CT data were generated from the CAD model at two different resolutions (0.25 and 0.5 mm).

We first conducted a pilot study where a single user (the first author) localized the fiducials in all three image sets (i.e., real and synthetic CT) and used two different tracking systems to digitize the fiducials on the phantom. We then performed a multi-user study where 10 subjects localized the fiducials in the CT image and digitized the fiducials using one tracking system. In all cases, the fiducials were localized in the image using 3D Slicer and were digitized using a tracked pointer. In all registration experiments, we used 8 fiducial markers for registration and then used the remaining 2 fiducials to compute the target registration error (TRE).

Pilot study

The single user localized the fiducials in the synthetic and real CT data using 3D Slicer. This provided three target point sets for the PPR method: one set from the synthetic CT with 0.25-mm resolution, one set from the synthetic CT with 0.5-mm resolution, and one set from the CT data. In addition, surface models were created and used in the model-based localization method, which provided the corresponding three target point sets for the PPRM and ICTP methods. Each image localization was performed 10 times.

The fiducial localization error (FLE) in the image is computed by comparing the localized fiducial positions with the ground truth fiducial positions. For the synthetic CT data, the ground truth fiducial positions are known because the synthetic CT coordinate system is the same as the CAD model coordinate system. For the real CT data, the ground truth is estimated by performing a paired-point registration between the CAD model and the CT data, using all 10 fiducials. The resulting transformation is used to convert the fiducial positions from the CAD model coordinate system to the CT coordinate system, which are then used as the (estimated) ground truth fiducial positions.

The source point sets are obtained using a digitizing probe tracked by commercially available optical trackers. One source point set was acquired using a fusionTrack 500 (Atracsys, Puidoux, Switzerland) that has a specified RMS accuracy of 0.09 mm, and another point set was acquired using a MicronTracker Hx40 (ClaroNav, Inc., Ontario, Canada) that has a specified RMS accuracy of 0.20 mm.

The user collected the source point sets in two different trials: *Experiment 1*-pick center of each fiducial marker as accurately as possible (best-case scenario) and *Experiment 2*-pick near boundary of each fiducial marker (worst-case scenario). Each trial was performed 20 times with two different tracking systems.

Multi-user study

A multi-user study was performed with institutional review board approval (HIRB00003967) and consisted of 10 sub-

jects (who are not surgeons), divided into two groups. *Group 1* was instructed to localize the fiducials as accurately as possible, whereas *Group 2* was instructed to localize them as efficiently as possible; this was intended to replicate the conditions of *Experiment 1* and *Experiment 2*, respectively. The target data set was collected on the CT data, and the source data set was collected using the fusionTrack 500.

Results

Model-based fiducial localization in image (pilot study)

Figure 6 shows the fiducial localization error (FLE) for each of the 10 fiducials, when localized manually and by the model-based localization method (stage 1 of the 3-stage registration procedure) in the 0.25-mm resolution synthetic CT data (top), the 0.5-mm resolution synthetic CT data (middle), and the CT data (bottom). The FLE is computed as the difference between the localized position and the ground truth, which is precisely known for the synthetic CT data and estimated for the real CT data as described in the "Pilot study" section. In the latter case, the registration between the fiducials in the CAD model and the CT image had a fiducial registration error (FRE) of 0.24 mm.

Although the user tried to accurately select the center points of each fiducial, the manual localization method has about 0.20- and 0.24-mm error with the 0.25- and 0.5-mm resolution synthetic CT data, respectively, and 0.43-mm error with the CT data. In contrast, the model-based fiducial marker localization method shows about 0.03- and 0.06-mm error with the 0.25- and 0.5-mm resolution synthetic CT data, and 0.23-mm error with the real CT data, which is a significant improvement over the manual method. The model-based method also produces more consistent results, as seen by the significantly lower standard deviation when compared to the manual method. This effectively makes fiducial localization user-independent, since the only effect of the user is in the choice of the initial center point (and possibly the initial normal). Although the FLE obtained with the real CT data (0.23 mm) appears to be much larger than with the synthetic CT data (0.03–0.06 mm), much of this may be due to the method used to estimate the ground truth, which yielded an FRE of approximately 0.24 mm.

Registration between image and tracking system

The residual error and TRE are compared using three different methods:

PPR: paired-point registration between intraoperatively digitized fiducials (Source points), P_S, and user-selected image fiducials (Target points), P_T.

Fig. 6 Comparison of fiducial localization error (FLE) between manual localization and model-based localization; the *top* and the *middle* results are from 0.25- and 0.5-mm resolution synthetic CT data, and the *bottom* results are from CT data. Each *bar* shows the mean and standard deviation of 10 trials for each of 10 fiducial markers; the *blue bars* are the result of manual localization, and the *red bars* are the result of model-based localization
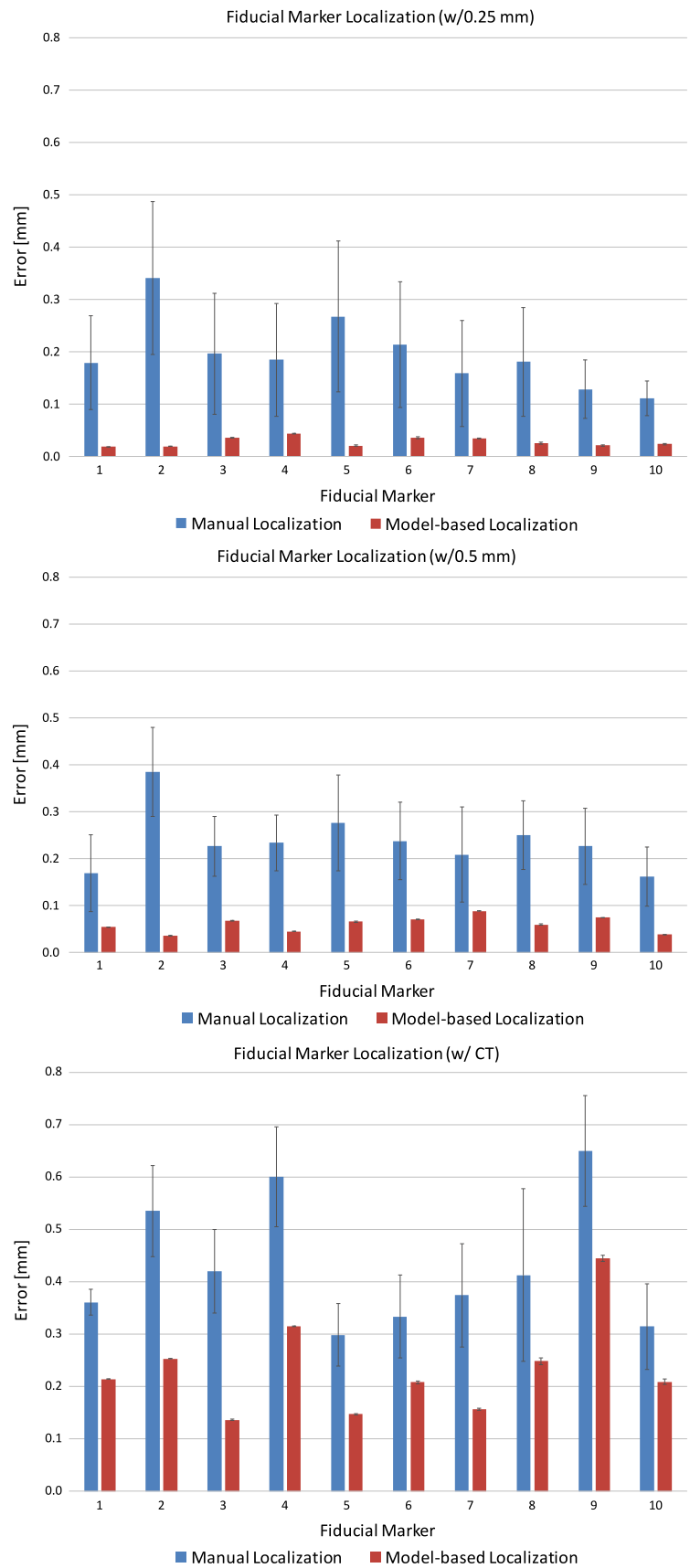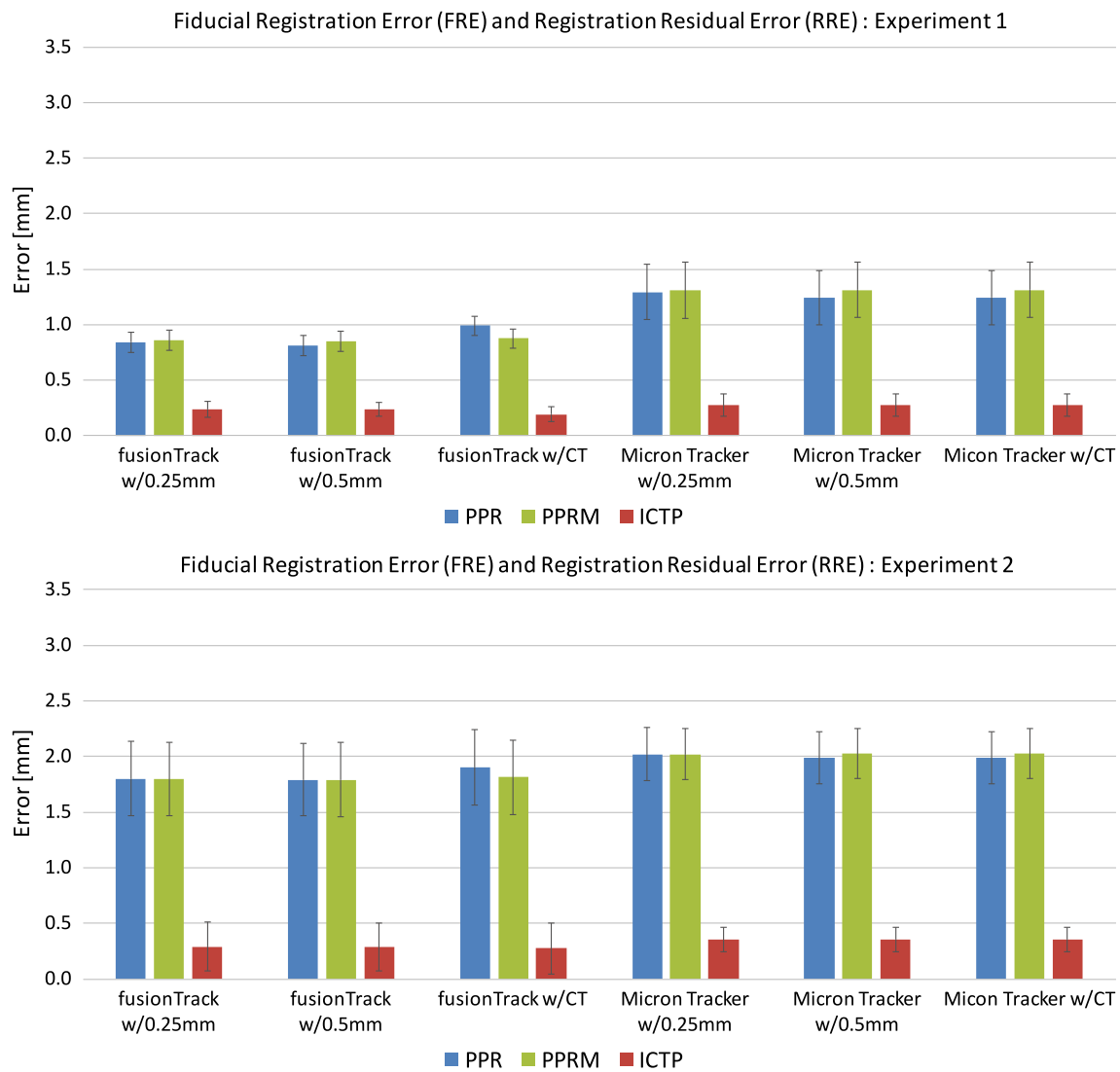
Fig. 7 FRE and RRE for Experiment 1 (*top*) and Experiment 2 (*bottom*) using two tracking systems, with three registration methods: PPR, PPRM, and ICTP (proposed method). Each *bar* shows the mean and standard deviation of 20 trials

PPRM: paired-point registration between intraoperatively digitized fiducials, P_S, and localized image fiducials using model-based localization (Localized Target), P_{LT}; this is also the initial registration for ICTP.

ICTP: ICP registration between intraoperatively digitized fiducials, P_S, and touchable region, S_{TR}, corresponding to each fiducial.

For PPR and PPRM, the residual error is represented by the fiducial registration error (FRE), which is the root-mean-square (RMS) error between the transformed source fiducials and the target fiducials. For ICTP, the registration residual error (RRE) is defined as the RMS error between the transformed source fiducials and the closest points in the touchable regions of the target fiducials.

Pilot study results

Figure 7 shows the FREs for PPR and PPRM, and RRE for ICTP, applied to the pilot study data collected with two tracking systems; the top graphs are the results from Experiment 1 (best-case scenario), and the bottom graphs show the results of Experiment 2 (worst-case scenario). Each bar shows the results (mean and standard deviation) of 20 trials. Not surprisingly, the proposed ICTP method has much lower residual error because the intraoperative points could be matched with any point in the touchable region, rather than a specific fiducial center point. Lower residual error does not necessarily mean better registration, however, so it is necessary to compare the TREs, which are shown in Fig. 8. As before, each bar shows the results (mean and standard deviation) of 20 trials. This figure shows that the proposed method has better
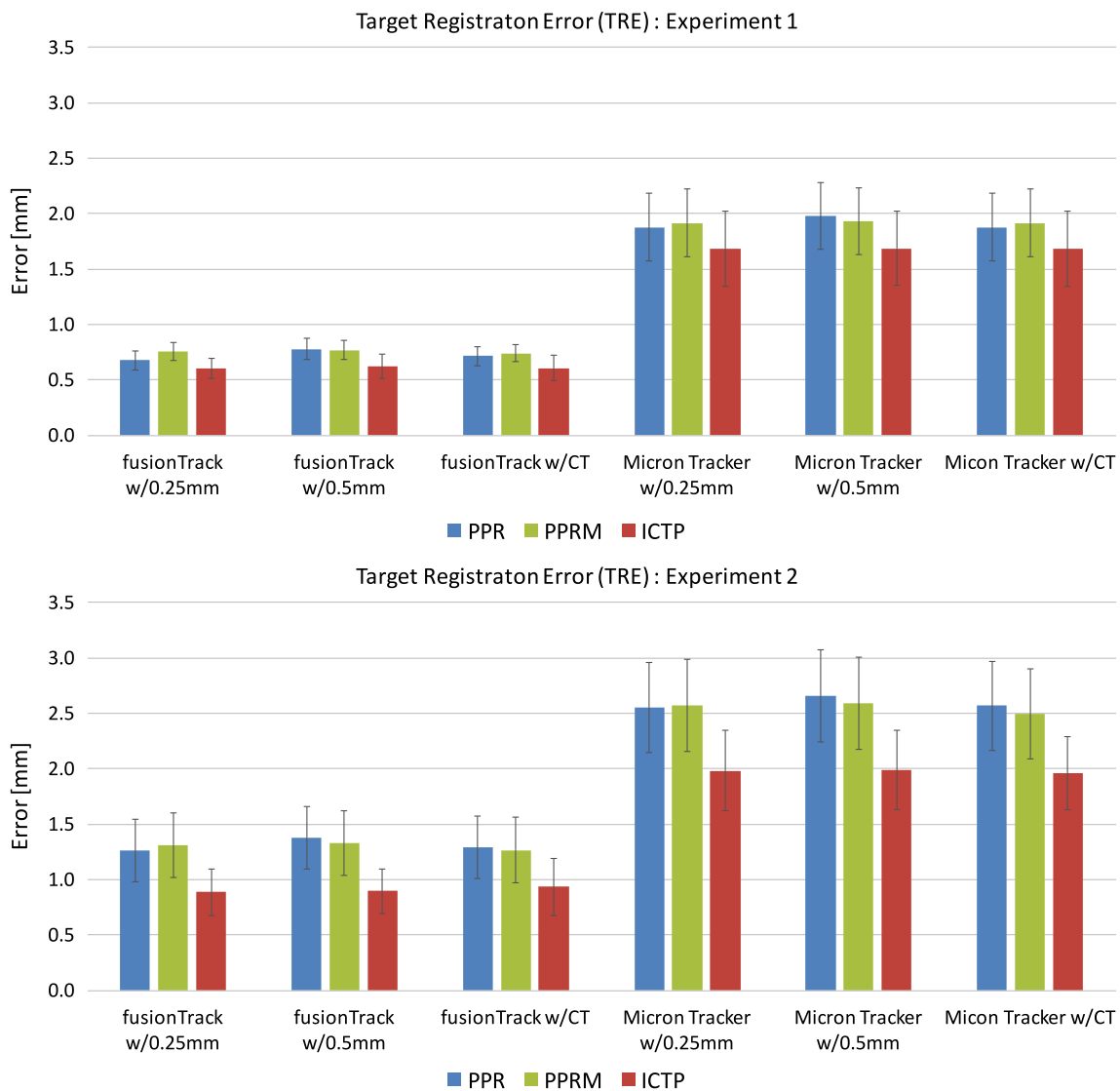
Fig. 8 TRE for Experiment 1 (*top*) and Experiment 2 (*bottom*) using two tracking systems, with three registration methods: PPR, PPRM, and ICTP (proposed method). Each *bar* shows the mean and standard deviation of 20 trials

Table 1 Results for Experiment 1, showing mean ± SD for FRE, RRE, and TRE; *p* values indicate probability that ICTP provides same performance (TRE) as PPRM or PPR (null hypothesis)

Tracker	Voxel (mm)	ICTP		PPRM			PPR		
		RRE (mm)	TRE (mm)	FRE (mm)	TRE (mm)	$p <$	FRE (mm)	TRE (mm)	$p <$
FusionTrack 500	0.25	0.24 ± 0.07	0.60 ± 0.09	0.86 ± 0.09	0.75 ± 0.08	0.001	0.84 ± 0.09	0.68 ± 0.09	0.01
	0.50	0.24 ± 0.06	0.62 ± 0.11	0.85 ± 0.09	0.77 ± 0.09	0.001	0.81 ± 0.09	0.78 ± 0.10	0.001
	CT	0.19 ± 0.07	0.61 ± 0.11	0.87 ± 0.09	0.74 ± 0.08	0.001	1.00 ± 0.09	0.72 ± 0.09	0.001
Micron Hx40	0.25	0.27 ± 0.10	1.68 ± 0.34	1.31 ± 0.25	1.92 ± 0.31	0.05	1.29 ± 0.25	1.88 ± 0.31	0.01
	0.50	0.27 ± 0.10	1.69 ± 0.34	1.31 ± 0.25	1.93 ± 0.30	0.05	1.24 ± 0.25	1.98 ± 0.30	0.01
	CT	0.26 ± 0.10	1.61 ± 0.33	1.27 ± 0.24	1.85 ± 0.31	0.05	1.27 ± 0.23	1.89 ± 0.30	0.01

performance than the other two methods. The FREs, RRE, TREs, and *p* values for Experiments 1 and 2 are summarized in Tables 1 and 2, respectively.

The ICTP method showed statistically significant differences compared to PPR and PPRM for synthetic and real CT and for both tracking systems. For both experiments, a *t* test

Table 2 Results for Experiment 2, showing mean ± SD for FRE, RRE, and TRE; p values indicate probability that ICTP provides same performance (TRE) as PPRM or PPR (null hypothesis)

| Tracker	Voxel (mm)	ICTP		PPRM			PPR		
		RRE (mm)	TRE (mm)	FRE (mm)	TRE (mm)	$p<$	FRE (mm)	TRE (mm)	$p<$
FusionTrack 500	0.25	0.29 ± 0.22	0.89 ± 0.21	1.80 ± 0.33	1.31 ± 0.29	0.001	1.80 ± 0.34	1.26 ± 0.28	0.001
	0.50	0.29 ± 0.22	0.90 ± 0.20	1.79 ± 0.33	1.33 ± 0.29	0.001	1.79 ± 0.33	1.38 ± 0.28	0.001
	CT	0.28 ± 0.23	0.93 ± 0.26	1.82 ± 0.34	1.27 ± 0.29	0.001	1.91 ± 0.34	1.29 ± 0.28	0.001
Micron Hx40	0.25	0.35 ± 0.11	1.98 ± 0.36	2.02 ± 0.23	2.57 ± 0.42	0.001	2.02 ± 0.24	2.55 ± 0.41	0.001
	0.50	0.36 ± 0.11	1.99 ± 0.36	2.03 ± 0.23	2.59 ± 0.42	0.001	1.99 ± 0.23	2.66 ± 0.41	0.001
	CT	0.36 ± 0.12	1.96 ± 0.33	2.01 ± 0.24	2.50 ± 0.41	0.001	2.01 ± 0.23	2.57 ± 0.40	0.001
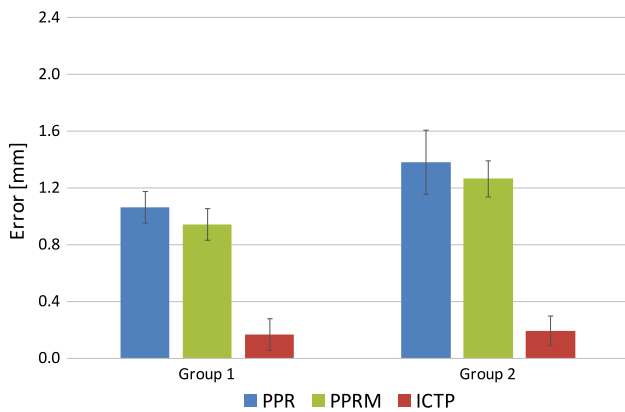
Fig. 9 FREs and RRE for Group 1 and Group 2 with three registration methods: PPR, PPRM, and ICTP (proposed method). Each *bar* shows the mean and standard deviation of 5 trials

Fig. 10 TRE for Group 1 and Group 2 with three registration methods: PPR, PPRM, and ICTP (proposed method). Each *bar* shows the mean and standard deviation of 5 trials
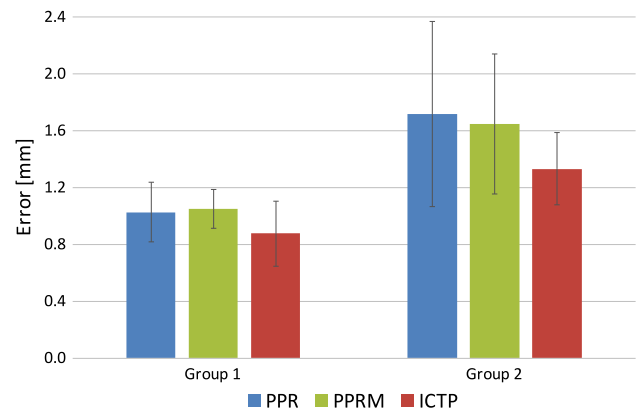
produced p values less than 0.05 when comparing TREs of the ICTP method to PPR or PPRM, regardless of the tracking system or CT data set. Experiment 2 showed a much larger improvement ($p < 0.001$ in all cases) than Experiment 1, as expected since it contained the intraoperative points that were poorly collected (i.e., far from the true fiducial centers).

Multi-user study results

Figure 9 shows the comparison of the RRE of the proposed method with the FREs of PPR and PPRM, and Fig. 10 presents the comparison of the TRE of ICTP with the TREs of PPR and PPRM. Due to the limited number of subjects (5 in each group), statistical analysis was not conducted.

As anticipated, the results for *Group 1* and *Group 2* of the multi-user study are comparable to the results for *Experiment 1* and *Experiment 2* of the single-user study, respectively. For both *Experiment 1* and *Group 1*, the emphasis was on accurate data collection; thus, the results show the best overall registration (lower TRE) for all methods and consequently a smaller improvement is obtained with the proposed ICTP method. In contrast, *Experiment 2* and *Group 2* relied on less accurate data; in *Experiment 2*, the single user intentionally

collected inaccurate data, whereas in *Group 2*, the 5 users were less careful because they were instructed to perform the task quickly. As a result, all methods produced less accurate registration results, but the proposed ICTP method yielded a more dramatic accuracy improvement with respect to the other two methods.

Discussion

The proposed method is designed to compensate for user errors in preoperative and intraoperative point collections, which are more likely when users manually localize the fiducial marker on the screen and when the digitizing tool does not precisely mate with a feature on the fiducial marker.

The first situation occurs in practice when users pick the fiducial points on the orthogonal views of the 3D image data, or on a 3D model that was generated from the 3D image data. As shown in Fig. 6, manual selection of the target point set introduces error even when a user attempts to carefully select the center point of the fiducial marker. The proposed model-based fiducial localization can improve the reliability, as shown in Fig. 6. While the model-based

method significantly reduces the FLE (Fig. 6), in our experiments, it had little effect on the residual error (Figs. 7, 9) and TRE (Figs. 8, 10). This is especially evident when comparing the PPR and PPRM methods, which differ only in that PPRM uses the model-based localization method. Generally, the residual error and TRE are similar, and in some cases, PPRM appears to produce a less accurate result. We hypothesize that this is due to cancellation of error; that is, the higher localization error obtained with PPR may be canceling other errors in the registration procedure. For the ICTP method, the model-based localization is more important because it is used to locate not just the fiducial center point, but also the orientation of the touchable region. As further verification, we applied the ICTP method without the model-based localization to the single-user data, using target points from the CT image and source points collected with the fusionTrack 500, and observed a small decrease in accuracy. Specifically, the TRE increased from 0.61 ± 0.11 to 0.70 ± 0.15 mm in Experiment 1 and from 0.93 ± 0.26 to 1.14 ± 0.33 mm in Experiment 2.

Errors in intraoperative point selection occur, for example, when a pointer probe is used to touch the center of a donut-shaped marker, such as the one shown in Fig. 2. Our phantom experiments did indeed show a larger improvement in registration accuracy when we intentionally performed a poor point collection (Experiment 2) or motivated the users to favor speed over accuracy (Group 2). This relative accuracy improvement was observed regardless of which tracking system was used to collect the intraoperative points.

For a brief mathematical analysis, consider N fiducials located at image coordinates $\overrightarrow{P_i}$, $i = 1, \ldots, N$. For simplicity, we consider only the translation component, $\overrightarrow{t}$, of the transformation. The fiducials digitized by the tracking system, $\overrightarrow{S_i}$, will have coordinates as follows:

$$\overrightarrow{S_i} = \overrightarrow{t} + \overrightarrow{P_i} + R_i^m [\Delta x_i, \Delta y_i, \epsilon_i]^T \qquad (4)$$

In this equation, R_i^m is the rotation of the coordinate system of marker i, where the z-axis corresponds to the normal and the x- and y-axes are the basis vectors for the touchable region. Thus, ϵ_i denotes a small error (e.g., due to tracking system inaccuracy), and Δx_i and Δy_i denote potentially larger errors due to poor intraoperative digitization (tracking system inaccuracy in these directions can be considered negligible in comparison or can be included in Δx_i and Δy_i).

For paired-point registration (PPR), the estimated translation component, $\overrightarrow{t}_{PPR}$, is computed by subtracting the centroid of the image points, $\overrightarrow{P_i}$, from the centroid of the tracking points, $\overrightarrow{S_i}$:

$$\overrightarrow{t}_{PPR} = \overrightarrow{t} + \frac{1}{N} \sum_{i=1}^{N} R_i^m [\Delta x_i, \Delta y_i, \epsilon_i]^T \qquad (5)$$

The above equation shows that with PPR, the estimated translation is corrupted by the potentially large digitization errors. For the proposed ICTP method, the analysis must consider the iterative nature of the algorithm. Specifically, the source points, $\overrightarrow{S_i}$, are transformed based on the current estimate of the transformation, and the closest points on the target model are found. In this case, the target model consists of the touchable regions. We consider the case where the iterative method is nearing convergence; specifically, when the estimate of the translation is within $\overrightarrow{\delta}$ of the true translation, in which case the source points are given by equation (4), with $\overrightarrow{t} = \overrightarrow{\delta}$. The closest points on the target are given by:

$$\overrightarrow{P_i}^{cp} = \overrightarrow{P_i} + R_i^m \left([\Delta x_i, \Delta y_i, 0]^T + \overrightarrow{\gamma_i} \right) \qquad (6)$$

Here, we introduced the (small) $\overrightarrow{\gamma_i}$ terms to account for the effect of the translation $\overrightarrow{\delta}$ and for small errors in the estimate of the rotation matrix R_i^m (which can be expressed by $R_i^m (I + \Omega)$, where Ω is a skew-symmetric matrix representing the small rotation error). Equation (6) also makes the assumption that $\overrightarrow{\delta}$ is small enough so that the transformed source points are within the bounds of the touchable region. As with Eq. (5), the incremental translation is given by subtracting the centroids:

$$\overrightarrow{\Delta t}_{ICTP} = \overrightarrow{\delta} + \frac{1}{N} \sum_{i=1}^{N} R_i^m \left([0, 0, \epsilon_i]^T - \overrightarrow{\gamma_i} \right) \qquad (7)$$

The above equation is nearly independent of the digitization errors, Δx_i and Δy_i; in reality, they make a minor contribution to $\overrightarrow{\gamma_i}$ due to small errors in the estimation of R_i^m. This analysis demonstrates that the proposed ICTP method is less sensitive to poor intraoperative digitization of the fiducials.

We further investigated the influence of the number and quality of fiducials. Figure 11 shows the mean TRE of the three registration methods as a function of the number of fiducials used for registration. All methods show a general trend where the accuracy improves as fiducials are added, until 6 or 7 fiducials are used, at which point adding fiducials provides little benefit. In addition, we tested different combinations of high-quality fiducials from Experiment 1 with low-quality fiducials from Experiment 2. Figure 12 presents the TREs corresponding to different ratios of low- and high-quality fiducials. This figure clearly shows that the proposed ICTP method produces consistent results that are nearly independent of the quality of the fiducials, whereas the accuracy of the PPR and PPRM methods degrades as more low-quality fiducials are used.

For the specific marker used in this study, an alternative strategy is to define a non-isotropic noise model that has a
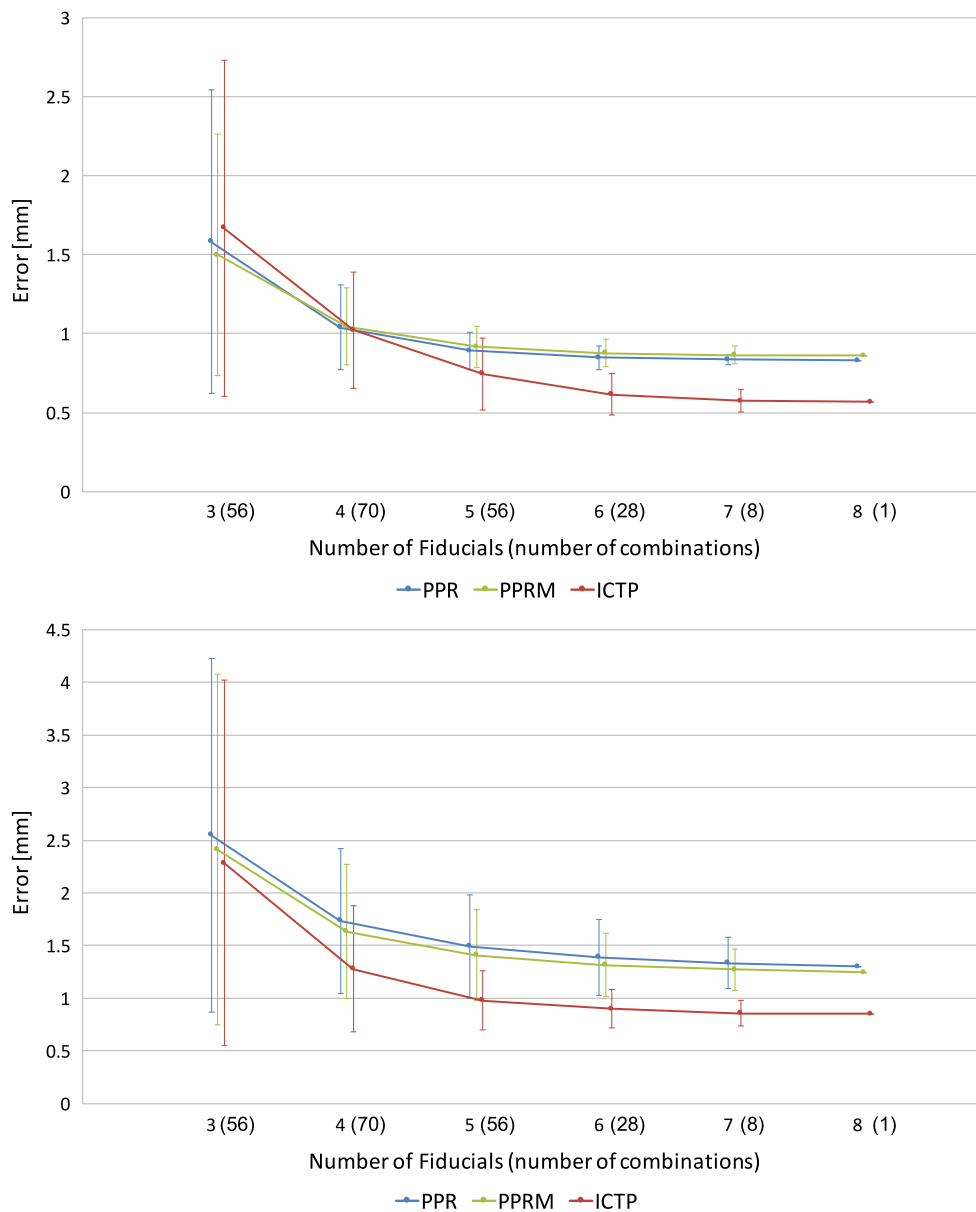
Fig. 11 TREs with different numbers of fiducials with three registration methods: PPR, PPRM, and ICTP (proposed method); the *top* shows the results with Experiment 1, and the *bottom* shows the results with Experiment 2. Each point includes the mean and the standard deviation of all combinations that contain the specified number of fiducials; the number of combinations is shown in parentheses. For visual clarity, small horizontal shifts were applied to separate the points

larger variance in the direction corresponding to our touchable region. We note, however, that our model-based method enables the definition of arbitrary touchable regions (e.g., cup-shaped regions), whereas non-isotropic noise models are difficult when not aligned with a Cartesian coordinate system. Also, it is still possible to incorporate a non-isotropic noise model in our method to handle an optical tracker (i.e., with larger variance in depth).

Conclusions and future work

We presented a new iterative point-based registration approach for surgical navigation and surgical robot systems that combines model-based fiducial localization with the paired-point and ICP registration methods using a touchable region model. The proposed ICTP registration framework shows improved accuracy without additional time-consuming or burdensome preoperative or intraoperative procedures. The
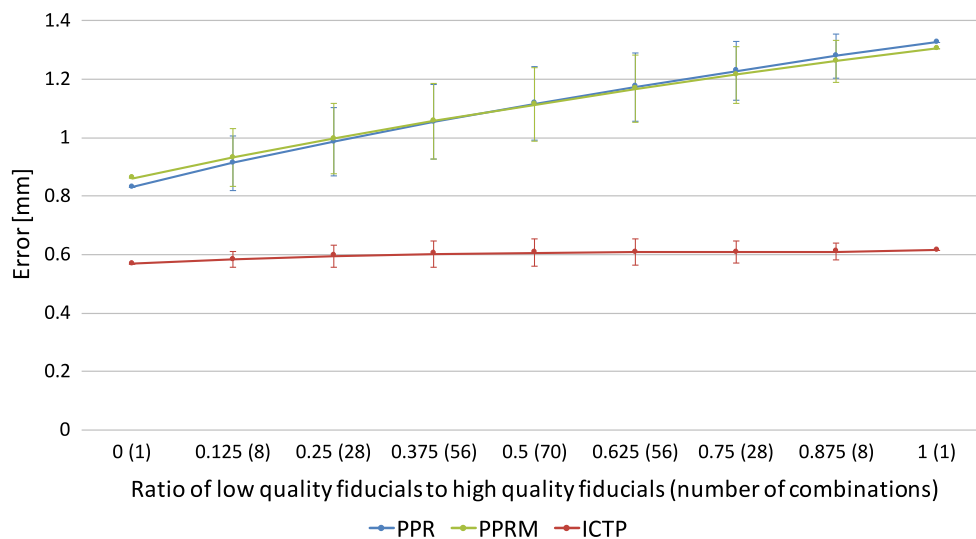
Fig. 12 TREs with different distributions of fiducials with three registration methods: PPR, PPRM, and ICTP (proposed method). The *horizontal axis* indicates the ratio of low-quality fiducials (from Experiment 2) to high-quality fiducials (from Experiment 1). The left-most point (0) corresponds to Experiment 1 (no low-quality fiducials), whereas the right-most point (8) corresponds to Experiment 2. Each point indicates the mean and the standard deviation of all combinations that produce the specified ratio; the number of combinations is shown in parentheses

experiments demonstrate that TREs of the proposed method are improved with respect to standard paired-point registration, whether the image points are selected by the user (PPR) or localized by a model-based method (PPRM). Most importantly, we achieved a much larger improvement in Experiment 2 of the single-user study, and in Group 2 of the multi-user study, which consisted of poorly collected intraoperative fiducial points. This could be beneficial in cases where surgeon unfamiliarity with a particular navigation or surgical robot system could lead to larger errors when selecting fiducials in the image data and/or digitizing them on the patient with a tracked tool. This may also save time in the operating room by reducing the need for the surgeon to recollect one or more fiducial points to correct for poor initial digitization.

As previously noted, we considered two important goals: (1) the registration framework must support the intraoperative workflow for point-based registration that is widely used in surgical navigation and surgical robotics and (2) the registration framework should produce significant improvement in the fiducial localization and registration, as compared to the conventional paired-point registration, especially when the user introduces large localization errors in either or both of the point sets. This study demonstrates that these goals have been achieved.

This study was performed with synthetic CT data generated from a CAD model of the phantom and real CT volume data. The synthetic CT data enable the ground truth target points to be defined from the CAD model, which is appropriate for evaluation of the registration method, and the real CT data enable to evaluate the proposed method in more realistic conditions.

Future work will address the complete workflow and evaluate the performance of the model-based fiducial localization method using a more realistic phantom or cadaver. Also, we plan to explore different fiducial markers with more complex touchable regions; this should include algorithms to offset the touchable region based on the radius of the digitizing probe. Finally, our registration method could incorporate a non-isotropic noise model for (at least) the tracking system and should be compared to recent methods that utilize a nonisotropic noise model to also characterize point collection error.

References

1. Arun K, Huang T, Blostein S (1987) Least-squares fitting of two 3-D point sets. IEEE Trans Pattern Anal Mach Intell 9(5):698–700

2. Besl PJ, McKay ND (1992) A method for registration of 3-D shapes. IEEE Trans Pattern Anal Mach Intell 14(2):239–256

3. Billings S, Kang HJ, Cheng A, Boctor E, Kazanzides P, Taylor R (2015) Minimally invasive registration for computer-assisted orthopedic surgery: combining tracked ultrasound and bone surface points via the P-IMLOP algorithm. Int J CARS 10(6):761–771

4. Fattori G, Riboldi M, Desplanques M, Tagaste B, Pella A, Orecchia R, Baroni G (2012) Automated fiducial localization in CT images based on surface processing and geometrical prior knowledge for radiotherapy applications. IEEE Trans Biomed Eng 59(8):2191–2199

5. Grimson W, Kikinis R, Jolesz F, Black P (1999) Image-guided surgery. Sci Am 280(6):54–61

6. Gu L, Peters T (2004) 3D automatic fiducial marker localization approach for frameless stereotactic neuro-surgery navigation. Med Imaging Augment Real 3150:329–336

7. Ma B, Ellis R (2003) Robust registration for computer-integrated orthopedic surgery: laboratory validation and clinical experience. Med Image Anal 7(3):237–250

8. Maurer CR Jr, Fitzpatrick JM, Wang MY, Galloway RL Jr, Maciunas RJ, Allen GS (1997) Registration of head volume images using implantable fiducial markers. IEEE Trans Med Imaging 16(4):447–462

9. Moghari MH, Abolmaesumi P (2007) Point-based rigid-body registration using an unscented kalman filter. IEEE Trans Med Imaging 26(12):1708–1728

10. Nagy DA, Haidegger T, Yaniv Z (2014) A framework for semi-automatic fiducial localization in volumetric images. Augment Environ Comput Assist Interv 8678:138–148

11. Perry J, Rosenbaum A, Lunsford D, Swink C, Zorub D (1980) Computed tomography-guided stereotactic surgery: conception and development of a new stereotactic methodology. Neurosurgery 7(4):376–381

12. Pieper SD, Halle M, Kikinis R (2004) 3D Slicer. In: IEEE International Symposium on Biomedical Imaging (ISBI), 15–18 April, Arlington, VA, USA. pp 632–635

13. Wang M, Song Z (2008) Automatic detection of fiducial marker center based on shape index and curvedness. Med Imaging Augment Real 5128:81–88

14. Wang M, Song Z (2009) Automatic localization of the center of fiducial markers in 3D CT/MRI images for image-guided neuro-surgery. Pattern Recognit Lett 30:414–420